nature neuroscience

A proportional but slower NMDA potentiation follows AMPA potentiation in LTP

Alanna J Watt[1,2], Per Jesper Sjöström[1,2], Michael Häusser[2], Sacha B Nelson[1] & Gina G Turrigiano[1]

Most excitatory glutamatergic synapses contain both AMPA and NMDA receptors, but whether these receptors are regulated together or independently during synaptic plasticity has been controversial. Although long-term potentiation (LTP) is thought to selectively enhance AMPA currents and alter the NMDA-to-AMPA ratio, this ratio is well conserved across synapses onto the same neuron. This suggests that the NMDA-to-AMPA ratio is only transiently perturbed by LTP. To test this, we induced LTP at rat neocortical synapses and recorded mixed AMPA-NMDA currents. We observed rapid LTP of AMPA currents, as well as delayed potentiation of NMDA currents that required previous AMPA potentiation. The delayed potentiation of NMDA currents restored the original NMDA-to-AMPA ratio within 2 h of LTP induction. These data suggest that recruitment of AMPA receptors to synapses eventually induces a proportional increase in NMDA current. This may ensure that LTP does not alter the relative contributions of these two receptors to synaptic transmission and information processing.

In primary sensory cortex, both AMPA receptors (AMPAR) and NMDA receptors (NMDAR) are the dominant contributors to excitatory synaptic currents, and sensory information is carried by activation of both receptor types[1,2]. At neocortical synapses, the ratio of current through these two receptor types remains nearly constant after early postnatal development[3], and during homeostatic synaptic plasticity AMPA and NMDA currents are scaled up and down proportionally[4]. Furthermore, careful measurement of the NMDA and AMPA components of individual quantal currents shows a strong correlation across synapses, suggesting that the ratio of the two receptor types is remarkably constant[4–7].

In contrast to the proportional regulation of AMPA and NMDA currents observed during homeostatic synaptic scaling, the prevailing model of LTP suggests that AMPAR-mediated currents are increased after potentiation, whereas NMDA currents are unaffected[8–13] (but see refs. 14–19). The considerable evidence for independent regulation of synaptic AMPA and NMDAR during LTP (for review, see ref. 20) raises the question of how a constant NMDA-to-AMPA ratio can be maintained at neocortical synapses in the face of ongoing synaptic plasticity. Whereas the independent regulation of AMPAR has been inferred from many studies of LTP, the amplitude of the NMDA currents has often been measured for only a short period after LTP induction[8–11]. We postulated that although LTP might initially perturb the NMDA-to-AMPA ratio, perhaps NMDA potentiation tracks AMPA potentiation, but on a slower time scale.

To examine this hypothesis, we induced a rapid, global LTP of AMPA miniature excitatory postsynaptic currents (mEPSCs) in cultured cortical pyramidal neurons, and then recorded the NMDA-to-AMPA ratio of mEPSCs at different time delays after the induction protocol. We observed a rapid and long-lasting potentiation of AMPA currents (AMPA-LTP), and a delayed but also long-lasting potentiation of NMDA currents (NMDA-LTP), which restored the original NMDA-to-AMPA ratio. A similar delayed but proportional NMDA-LTP was observed at unitary connections between layer-5 pyramidal neurons in visual cortical slices. These data indicate that a stable NMDA-to-AMPA ratio is actively maintained at neocortical synapses in the face of ongoing plasticity.

RESULTS

Experiments were performed on cultured neocortical pyramidal neurons after 7–8 days *in vitro*, or on layer-5 pyramidal neurons in slices of visual cortex from postnatal day (P)14–18 rats. Pyramidal neurons in culture were visually identified as previously described[4,21,22]. Mixed AMPA-NMDA mEPSCs[4] or unitary excitatory EPSCs[23] were recorded as previously described.

Rapid AMPA and delayed NMDA potentiation

To measure the NMDA-to-AMPA ratio of quantal currents for several hours after the induction of LTP, we potentiated a large number of inputs onto cultured cortical pyramidal neurons by bath-application of a solution that induces correlated bursts of spiking in nearby neurons and strongly activates synaptic NMDAR (**Fig. 1a**)[13,24]. This involved a 15-min exposure to a solution with lowered external Mg^{2+}, containing bicuculline to partially block $GABA_A$-mediated inhibition, and with a concentration of glycine that saturates the NMDAR binding site[13].

This induction protocol was done on sister cultures in parallel; normal neuronal medium was then replaced and the cultures were returned to the incubator for different time durations until electrophysiological recordings were taken. Physiological recordings were done no longer than 1 h after a dish was removed from the incubator, and each neuron was assayed at only one time point. Mixed AMPA-

[1]Department of Biology and Volen National Center for Complex Systems, MS 08, 415 South Street, Brandeis University, Waltham, Massachusetts, 02454 USA. [2]Wolfson Institute for Biomedical Research and Department of Physiology, University College London, Gower Street, London WC1E 6BT, UK. Correspondence should be addressed to G.G.T. (turrigiano@brandeis.edu).

Published online 28 March 2004; doi:10.1038/nn1220

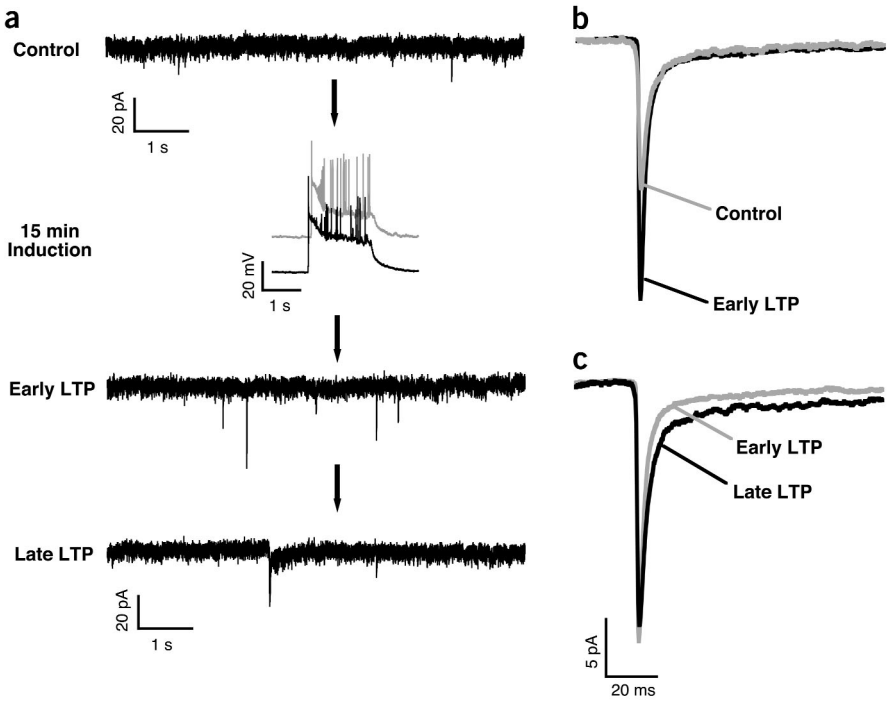

Figure 1 Long-term potentiation of mEPSCs. (**a**) Sample traces from voltage-clamp recordings from control (top) and potentiated neurons (bottom two traces). At this time-base, mEPSCs appear as rapid downward current deflections. Immediately after LTP induction (early LTP), AMPA quantal amplitude and mEPSC frequency increased. At times > 2 h after LTP induction (late LTP), both the AMPA and NMDA components of the mEPSC increased in amplitude, whereas mEPSC frequency returned to control levels. Inset: simultaneous recordings from two pyramidal neurons showing the correlated burst-like activity elicited by the induction medium. Gray trace has been offset on the voltage axis to aid visualization. (**b**) Average mEPSC waveforms from control (gray) and early LTP (black) showing that the rapid AMPA component of the mEPSC was potentiated (AMPA-LTP), whereas the slowly decaying NMDA component was unaffected. (**c**) Average mEPSC waveforms from early LTP (gray) and late LTP (black). During late LTP, potentiation of the NMDA component (NMDA-LTP) was now also evident.

NMDA-mediated mEPSCs were then recorded at –60 mV holding potential in artificial cerebrospinal fluid (ACSF) containing 0.05 mM $MgSO_4$, which greatly reduced the voltage-dependent block of the NMDAR and revealed a mixed AMPA-NMDA current at this holding potential. Because the AMPA and NMDA components of the mEPSCs recorded under these conditions have distinct time courses (AMPA peaks early and decays to baseline within 15 ms; NMDA peaks after 15 ms and decays with a time constant of ~150 ms, **Fig. 1b**), the amplitude of the two components can be determined by measuring at different time points as previously described[4].

Comparing the amplitude of the AMPA component of mEPSCs in control and potentiated sister cultures revealed that robust LTP (**Fig. 1b**, at least 120% of control values) was induced in approximately 80% of experiments. Unsuccessful LTP generally occurred if cultures were sparse, and it was probably due to differences in the level of activity induced by the potentiation protocol. When LTP occurred, it occurred reliably in all sister cultures within a given experiment. Because we wished to know what happened to the NMDA component of mEPSCs when the AMPA component was potentiated, we analyzed only those experiments in which LTP of

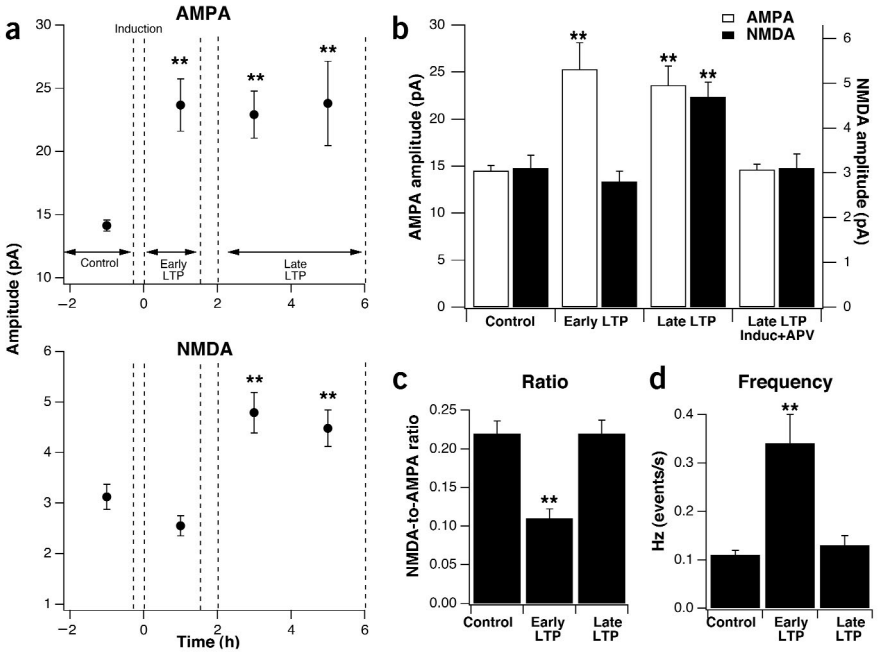

Figure 2 Delayed NMDA-LTP restores the NMDA-to-AMPA ratio. (**a**) Time-course of AMPA-LTP and NMDA-LTP. Top: AMPA-LTP occurred rapidly and was long-lasting without significant run-down. Bottom: NMDA-LTP occurred after a delay of 2 h and was also long-lasting. Time after induction was measured from the end of the induction period. Time points were binned as follows: 0–1.5 h, 2–3.5 h and 3.5–8 h. (**b**) Summary data comparing AMPA (white bars) and NMDA (black bars) synaptic currents from control, early LTP and late LTP recordings. Late LTP induction + APV had 200 μM DL-APV included in the induction solution, and was assayed 2–9 h after the induction. Neither AMPA nor NMDA currents were significantly different from controls, but they were both different from late LTP. (**c**) Average NMDA-to-AMPA ratios from control, early and late LTP. (**d**) LTP induction transiently enhances mEPSC frequency. mEPSC frequency increased ~3-fold during early LTP, but returned to controls levels by late LTP. $^{**}P < 0.0001$ compared to control. For this and subsequent figures, all error bars represent standard error of the mean.

AMPA currents was successfully induced. Potentiation of AMPA-mediated mEPSCs (AMPA-LTP) occurred as rapidly as could be measured (within minutes of potentiation) and lasted as long as was measured (up to 8 h; **Fig. 1c**). On average, AMPA currents were potentiated to 165 ± 9% of control values (n = 20 for control and 33 for LTP, $P < 0.0001$).

Table 1 Effects of potentiation on mEPSC kinetics and cellular properties

Condition	Rise time (ms)	τ_{NMDA} (ms)	R_s (MΩ)	R_{in} (MΩ)	V_m (mV)
Control (n = 20)	1.30 ± 0.05	176.1 ± 25.9	11.2 ± 0.7	227.8 ± 37.4	–63.8 ± 2.0
Early LTP (n = 14)	0.81 ± 0.05**	149.4 ± 38.5	12.6 ± 0.9	234.7 ± 38.4	–59.1 ± 1.4
Late LTP (n = 18)	1.04 ± 0.06**	174.1 ± 32.1	11.3 ± 0.5	196.4 ± 17.5	–59.4 ± 1.7

Average mEPSC 20–80% rise times, NMDA decay time constants (τ_{NMDA}), series resistances (R_s), resting membrane potentials (V_m) and input resistances (R_{in}) for neurons in each condition. Control (n = 20), early LTP ≤ 1.5 h after induction (n = 15), late LTP ≥ 2 h after induction (n = 18) (**$P < 0.0001$ compared to control).

Many researchers have found that LTP induction alters the NMDA-to-AMPA ratio[8–10]. Consistent with this, the NMDA component of mEPSCs was unchanged within the first 1.5 h of LTP induction (early LTP, n = 14, not different from control, n = 20), and the NMDA-to-AMPA ratio decreased (**Figs. 1b** and **2a,b**). By 2 h after LTP induction (late LTP, n = 18), however, the NMDA component of mEPSCs was potentiated (NMDA-LTP) and remained at this elevated level for as long as was measured (**Fig. 2a,b**; up to 8 h, significantly different from control, $P < 0.0005$). The late NMDA-LTP was closely matched in magnitude to the AMPA-LTP so that the NMDA-to-AMPA ratio was restored (**Fig. 2c**). Blocking NMDAR with the competitive antagonist APV during the induction period prevented both AMPA-LTP (**Fig. 2b**; 103 ± 4% of control values, n = 10) and the delayed NMDA-LTP (**Fig. 2b**; 101 ± 10% of control values), indicating that potentiation of both components of excitatory synaptic transmission required NMDAR activation during the induction period.

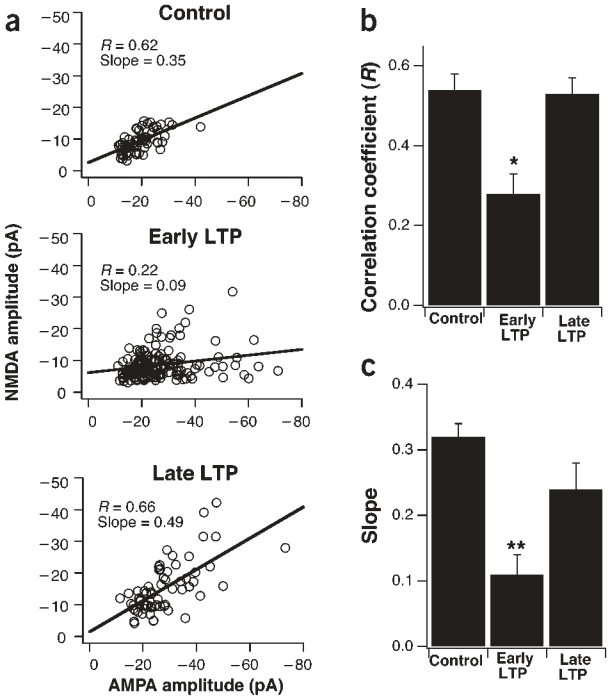

Figure 3 Correlation between the AMPA and NMDA amplitudes of individual mEPSCs. (**a**) Sample data from three representative neurons showing the correlation between the NMDA (y-axis) and AMPA (x-axis) components of individual mEPSCs from a control neuron (top), a neuron within 1.5 h of LTP induction (early LTP, middle) and a neuron more than 2 h after LTP induction (late LTP, bottom). Correlation coefficients (R) and slopes from the linear regression fit (solid line) are indicated. (**b**) Average R from control, early LTP and late LTP neurons. During early LTP, the correlation was significantly reduced, but increased again >2 h after induction. (**c**) Average slopes from linear regression fits of the correlation data. The average slope from early LTP was significantly different from control and not significantly different from zero, whereas control and late LTP slopes were not significantly different from each other but significantly different from slope = 0. *$P < 0.05$, **$P < 0.0001$, compared to control.

LTP transiently enhanced mEPSC frequency

In addition to the effects on AMPA and NMDA mEPSC amplitude, the induction of LTP was accompanied by a 310 ± 54% increase in mEPSC frequency (**Fig. 2d**, $P < 0.0005$) as has previously been observed[13,25–27]. However, the increase in mEPSC frequency was short-lived, and by 2 h after induction (late LTP), mEPSC frequency was indistinguishable from control (118 ± 18% of control values; $P > 0.05$). Given that immunohistochemistry has identified few silent synapses (<10% of excitatory synapses) on these neurons[22], these data suggest a transient presynaptic effect of the LTP protocol on the probability of spontaneous vesicle fusion.

A ~40% acceleration in mEPSC rise time was observed after LTP induction ($P < 0.0001$; **Table 1**). Changes in AMPAR subunit composition have been shown to change AMPAR decay[28,29], but not (to our knowledge) rise-time kinetics. The change in rise time is consistent with a presynaptically mediated enhancement of cleft glutamate concentration[30], which could result from a change in the kinetics of the fusion pore formation[31]. Whatever the source, the decrease in rise times was shorter-lived than the increase in AMPA amplitude, and it was 50% reversed in the late LTP condition even though AMPA amplitude remained elevated. Electrophysiological properties of the neurons (input resistance and resting membrane potentials) were not significantly different between control and LTP groups, nor were there any significant differences in the decay time constants of the NMDAR currents across conditions (**Table 1**).

The NMDA-to-AMPA ratio was regained at individual synapses

The average NMDA-to-AMPA ratio of mEPSCs was regained after initially being perturbed after LTP induction (**Fig. 2c**). We wondered if this was reflected in proportional changes in the AMPA and NMDA components of individual mEPSCs. To address this, we measured the peak AMPA and NMDA components of individual mEPSCs, as described previously[4]. We plotted the AMPA peak against the NMDA peak for each mEPSC from a given neuron and measured the coefficient of correlation (R) and the slope of this relationship. For control neurons, AMPA and NMDA amplitudes co-varied significantly at individual synapses (**Fig. 3a,b**; n = 12, slope significantly different from zero, $P < 0.005$). Within 1.5 h of LTP induction (early LTP), this correlation was reduced (**Fig. 3a,b**; n = 14, significantly different from control, $P < 0.005$; slope not different from zero, $P > 0.05$). However, after 2 h, the correlation increased again (**Fig. 3a,b**; n = 16, not significantly different from control, $P > 0.05$; slope different from zero, $P < 0.05$). In addition, the slope values decreased during early LTP, but returned close to control values during late LTP (**Fig. 3c**). These data

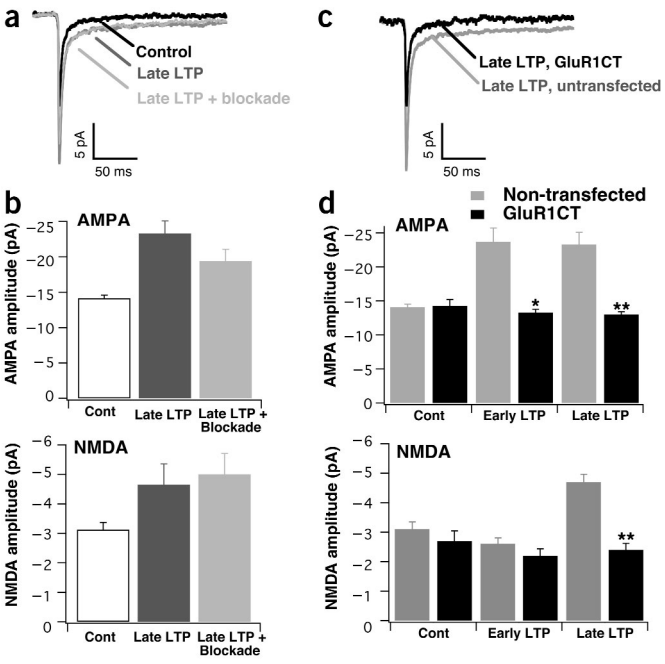

Figure 4 Delayed NMDA-LTP does not require post-induction activity or glutamate receptor activation, but requires AMPA-LTP. (**a**) Average mEPSCs from control (black trace), late LTP (dark gray trace), and neurons in which activity and glutamate receptors were blocked with TTX, DNQX and APV from immediately after induction until recording (late LTP + blockade, light gray trace). (**b**) Summary data for control ($n = 6$), late LTP ($n = 5$) and late LTP + blockade ($n = 7$) for AMPA (top) and NMDA (bottom) amplitudes. Late LTP + blockade was not significantly different from late LTP. (**c**) Average mEPSCs from untransfected neurons (gray trace) and from neurons expressing a GluR1CT construct (black trace). (**d**) Summary data showing AMPA (top) and NMDA (bottom) amplitudes for each condition. Nontransfected neurons in gray: control ($n = 7$), early LTP ($n = 4$) and late LTP ($n = 5$). GluR1CT-transfected neurons in black: control ($n = 6$), early LTP ($n = 5$) and late LTP ($n = 7$). Comparing GluR1CT-transfected neurons to non-transfected cells in the same condition, $^*P < 0.02$, $^{**}P < 0.006$, compared to control.

suggest that at the level of individual synapses, the original NMDA-to-AMPA ratio is restored 2 h after potentiation.

NMDA-LTP requires previous AMPA-LTP

LTP of AMPA currents might produce altered activity patterns and enhance glutamate receptor activation during the post-induction delay. To test whether this activity is required for the potentiation of NMDA currents, we pharmacologically blocked glutamatergic transmission and spike-dependent activity (with DNQX, APV and tetrodotoxin (TTX)) from the time point immediately after induction until recording >2 h later. This had no significant effect on late AMPA-LTP (**Fig. 4a**; different from control, $P < 0.02$, but not from late LTP) or on NMDA-LTP (**Fig. 4a,b**; different from control, $P < 0.01$, but not from late LTP). To determine whether NMDA-LTP depends upon the prior potentiation of AMPA currents, we used a green fluorescent protein (GFP)-tagged carboxy terminal of the GluR1 AMPAR subunit to block LTP of AMPA currents[32]. A GFP-tagged GluR1 carboxy terminal construct (GluR1CT) was expressed at low efficiency[22] and we recorded from transfected and nearby control neurons in the same dish after LTP induction. Overexpression of GluR1CT for 18 to 36 h had no significant effect on basal synaptic transmission (**Fig. 4c,d**), but completely blocked AMPA-LTP as previously described[33] (**Fig. 4c,d**, AMPA; early LTP GluR1CT significantly different from early LTP non-transfected, $P < 0.02$; late LTP GluR1CT significantly different from late LTP non-transfected, $P < 0.006$). Interestingly, the late NMDA–LTP was also completely blocked by GluR1CT (**Fig. 4c,d**; NMDA; late LTP GluR1CT significantly different from late LTP non-transfected, $P < 0.001$). These data suggest that potentiation of NMDA currents requires the prior potentiation of AMPA currents.

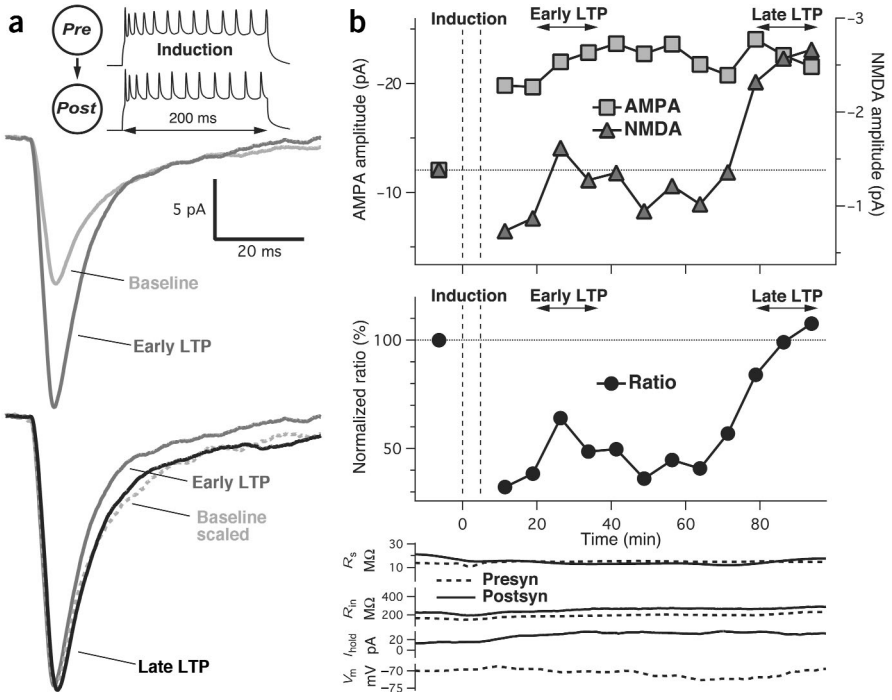

Figure 5 Delayed and proportional NMDA-LTP at a unitary connection between layer 5 pyramidal neurons. (**a**) Top: typical LTP induction protocol pairing pre- and postsynaptic firing. Bottom: average EPSC traces from the experiment shown in **b** (measured at time points indicated in **b**). Top traces show baseline (light gray) and early LTP (dark gray); robust AMPA-LTP was evident while the NMDA component was unchanged. Bottom traces illustrate early LTP (dark gray) and late LTP (black) where NMDA-LTP was evident. The scaled baseline (light gray, dashed line) was scaled to the AMPA peak of the late LTP. (**b**) Time course of example experiment. Top plot: the AMPA component of the EPSC showed rapid and persistent LTP, whereas the NMDA component did not potentiate until long after the induction. Bottom plot: the NMDA-to-AMPA ratio initially decreased following the induction, and subsequently recovered. The pre- and postsynaptic series resistances (R_s), input resistances (R_{in}), presynaptic V_m and postsynaptic holding current (I_{HOLD}) are shown below for the duration of the experiment.

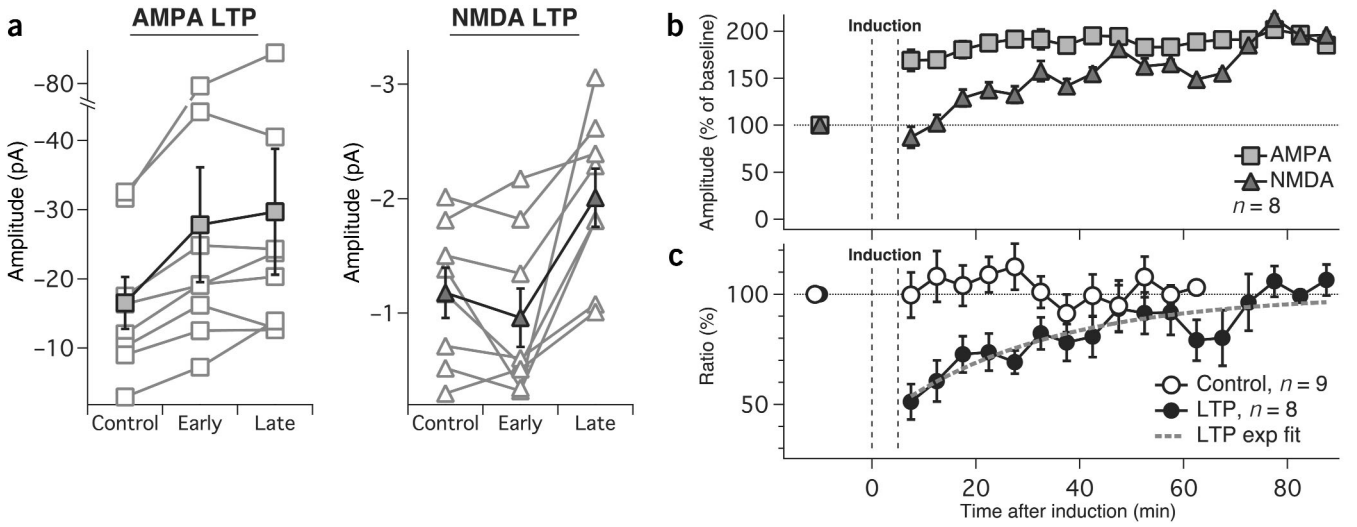

Figure 6 Summary data from layer-5 unitary synapses. (**a**) Summary of early and late LTP for AMPA and NMDA amplitudes, showing all 8 LTP experiments. Each recording is represented as a gray symbol connected by gray lines, and the average response amplitude is represented as a black symbol connected by black lines. (**b**) Ensemble data showing the normalized AMPA (open boxes) and NMDA (filled triangles) amplitudes over time for the 8 recordings in which LTP was induced. (**c**) Ensemble plot of the NMDA-to-AMPA ratio over time, for LTP experiments (filled circles) and control recordings (open circles). The dashed black line is an exponential fit to the LTP data; $\tau = 31$ min.

Delayed NMDA-LTP at unitary L5 pyramidal neuron synapses

To determine whether standard LTP protocols used in visual cortical slice preparations[23] also produce a delayed NMDA-LTP, we obtained paired whole-cell recordings between nearby, large layer-5 pyramidal neurons from rat (P14–18) primary visual cortex. We have previously shown that robust LTP can be induced at these unitary connections[23]. Synaptic strength was monitored by activation of single presynaptic action potentials at low frequencies (0.1–0.2 Hz), whereas the postsynaptic neuron was maintained in voltage clamp under conditions where the NMDA component of unitary EPSCs could be monitored, and LTP was induced by pairing pre- and postsynaptic firing (**Fig. 5a**). This induced immediate AMPA-LTP (to 168 ± 18% of control, $P < 0.007$, $n = 8$), which persisted throughout the experiment (**Figs. 5** and **6**). In contrast, NMDA currents were not significantly affected immediately after induction (86 ± 16% of control), but were significantly potentiated by 50 min after induction ($P < 0.006$; **Figs. 5** and **6**). Normalized ensemble data shows the average time course of the change in AMPA and NMDA amplitude and in the NMDA-to-AMPA ratio: immediately after LTP, the ratio dropped to about 50% of control (LTP different from control, $P < 0.0004$) and then slowly returned to control values (**Fig. 6b,c**; exponential fit, $\tau = 31$ min). In control experiments where no LTP was induced, the NMDA-to-AMPA ratio remained stable (**Fig. 6c**, $n = 9$), and there was no significant change in AMPA or NMDA amplitude during the course of the control recordings (AMPA = 101 ± 5% of baseline, NMDA = 106 ± 11% of baseline).

Interestingly, the NMDA potentiation observed at these unitary connections was faster than that observed in culture. Whereas in culture no significant NMDA potentiation was observed within the first 90 min after LTP, in our slice recordings on average the ratio was not significantly different from baseline by 45–55 min after LTP induction (**Fig. 6c**). This could reflect a faster process at layer-5 synapses than at the mixed excitatory synapses sampled in culture, or a difference in the state of the synapses in the two preparations. In either case, these data indicate that LTP induced by very different methods in very different preparations of neocortical neurons produces the same phenomenon: rapid AMPA-LTP and delayed but proportional NMDA-LTP.

DISCUSSION

There is considerable evidence that synaptic AMPAR and NMDAR number and distribution can be independently regulated by activity[34–41]. Measurements of the NMDA-to-AMPA ratio soon after LTP induction have consistently shown that this ratio is altered[11–13]. In keeping with this, we found that the AMPA component of excitatory transmission was selectively potentiated and the NMDA-to-AMPA ratio decreased soon after LTP induction. Surprisingly, measurement of the NMDA component 1–2 h or longer after LTP revealed a delayed increase that closely matched the AMPA potentiation, and restored the original NMDA-to-AMPA ratio. These results suggest that there is an active mechanism at neocortical synapses that preserves the relative contribution of AMPAR and NMDAR to synaptic transmission, despite dynamic regulation of overall synaptic strength.

The ability of LTP induction protocols to potentiate NMDA currents at hippocampal synapses has been controversial. Whereas some studies have observed NMDA-LTP[14–19], many others have not[8–13,20]. If a similar delayed NMDA-LTP occurs at hippocampal synapses, this could account for some of the discrepancies in the literature. Because the delayed NMDA-LTP is proportional to the AMPA-LTP, the ratio of current through these two receptor types is restored after a delay of one or more hours. This provides a resolution to two seemingly contradictory observations: (i) that AMPAR can be independently inserted following LTP, which should result in very different NMDA-to-AMPA ratios at different synapses[13,24,36] and (ii) that the NMDA-to-AMPA ratio is highly conserved across synapses onto individual cortical neurons of a given type[3–5]. Our data suggest that if *in vivo* LTP is ongoing and induces synapse-specific changes in synaptic strength, this will transiently alter the NMDA-to-AMPA ratio at particular synapses, but over time NMDA will 'catch up' and the ratio at each synapse will be restored. Early LTP may thus contribute some noise to the NMDA-to-AMPA ratio measured across individual mEPSCs (**Fig. 3**), but will not result in a progressive alteration in this ratio.

The GluR1CT construct has been suggested to prevent LTP by blocking the insertion of AMPAR into synapses[42]. Blocking AMPA-LTP with this construct also prevented NMDA-LTP, suggesting that AMPAR insertion may in turn induce a proportional increase in NMDA current. This could occur through a long-lasting modification in existing synaptic NMDAR properties, or through the recruitment of AMPAR-associated scaffolding proteins that increase synaptic NMDAR accumulation. The same mechanism could account for proportional changes in AMPA and NMDA currents during homeostatic synaptic scaling, so that slow changes in the accumulation of synaptic AMPAR[21,37,38] lead to proportional changes in NMDA currents[4].

If NMDAR potentiation is coupled to AMPAR insertion, why does it occur more slowly? One possibility is that there is a delayed generation of some limiting factor necessary for modification or synaptic recruitment of NMDAR—possibly alterations in the composition of NMDAR themselves[43]. Another speculative but interesting possibility is that NMDA-LTP accompanies the subunit-specific turnover of AMPAR. At hippocampal synapses, AMPA-LTP involves the insertion of GluR1/GluR2-containing receptors, which are subsequently replaced with GluR2/GluR3-containing AMPAR[42,44]. Since different AMPAR subunits interact with different scaffolding proteins[45,46], these new AMPAR might be accompanied by the scaffolding proteins that recruit additional NMDA current. This model suggests that a fixed stoichiometry in binding proteins in the postsynaptic density underlies the long-term maintenance of the NMDA-to-AMPA ratio at synapses.

One question raised by these results is whether the lag in NMDAR-LTP is important for synaptic function. NMDA-LTP is likely to enhance the destabilizing properties of Hebbian plasticity[47] because the additional NMDAR-mediated calcium influx at the synapse is predicted to enhance the ease with which further LTP can be induced. This effect could be mitigated to some extent by the delay in NMDA-LTP, as this delay will ensure that NMDA-LTP does not occur until well after the original potentiating event. It is interesting to note that the direction of change in NMDA current we observed here is opposite from that predicted by the BCM model, which predicts that LTP should reduce NMDA currents to raise the threshold for inducing LTP[48]. On the other hand, the slower, homeostatic and proportional adjustment of AMPA and NMDA currents observed previously[4] is in the right direction to counteract the destabilizing effects of AMPA and NMDA-LTP.

Excitatory synaptic strength is often equated with the size of the AMPA EPSC. However, both AMPAR and NMDAR contribute to information transfer at synapses, and the relative contribution of these two receptors will affect the voltage-dependence of transmission and the degree of temporal summation, both of which can have important consequences for circuit function[1,2]. The delayed NMDA-LTP means that the information transmitted by synapses will vary in the hours following potentiation. However, over longer time scales, the proportional regulation of AMPA and NMDA currents may ensure that Hebbian plasticity does not alter the relative contributions of these two receptor types to synaptic transmission and information processing.

METHODS

Culture experiments. All methods were approved by the Brandeis Animal Use Committee and were in accordance with National Institutes of Health guidelines. Visual cortical cultures were prepared from P3–4 rat pups, and whole-cell mEPSC recordings were obtained as previously described[4,22,49] using low-magnesium (0.05 mM) ACSF and voltage-clamp to –60 mV. LTP was induced by incubating the neurons at 37 °C and 5% CO_2 for 15 min in ACSF containing the following: NaCl, 126 mM; KCl, 5.5 mM; $MgSO_4$, 0.4 mM; NaH_2PO_4, 1 mM; $NaHCO_3$, 25 mM; $CaCl_2$, 2 mM; dextrose, 14 mM; glycine, 0.2 mM; bicuculline, 0.01 mM. Then, we replaced the medium in the culture dishes and returned them to the tissue culture incubator until recording. For post-induction blockade experiments, culture medium contained 1 μM TTX, 40 μM DNQX and 200 μM D-APV added upon replacement. Neurons were transfected with a GluR1CT-GFP construct with a Helios gene gun as previously described[22,49] between 16–24 h before the induction was performed.

Slice experiments. Paired whole-cell recordings from thick-tufted L5 neurons in 300 μm slices of rat (P14–18) visual cortex were performed as previously described[23], using low-magnesium (0.5 mM) ACSF. Postsynaptic neurons were voltage-clamped to –65 mV, or in some experiments to –50 mV to facilitate measurement of NMDA currents; in the latter case, the endocannabinoid inhibitor AM251 (1 μM, Tocris Cookson Inc.) was added to the ACSF to prevent LTD induction[50]. LTP was induced in current-clamp mode by pairing 200-ms pre- and postsynaptic current injections (0.9–1.2 nA) 30 times at 0.1–0.2 Hz. Recordings were not included if the post-pairing period was shorter than 50 min, or if the amount of LTP was not >1%. Early LTP was defined as the first 5 min after LTP induction, and late LTP as the last 5 min of each recording. AMPA and NMDA amplitudes were determined as previously described[3], except that for NMDA we used a window 30–60 ms after the presynaptic spike; longer or shorter windows did not affect the results. To illustrate the ensemble time-course of AMPA and NMDA LTP, the initial degree of potentiation for each recording was normalized to the initial average amount of potentiation. Recordings were terminated if input resistance (R_{in}) changed by more than 30%, resting membrane potential (V_m) changed by more than 8 mV, or series resistance (R_s) changed by more than 50%. Connections smaller than 3 pA were not used.

Statistics. All data are reported as mean ± s.e.m. for the number of neurons indicated. Statistical comparisons were performed using unpaired, two-tailed *t*-tests; for multiple comparisons, we used single-factor ANOVAs followed by Fisher's LSD tests or the Bonferroni-Dunn method; *P* values reflect the results of the post-hoc Fisher LSD tests. For all multiple comparisons in which statistical significance is reported, ANOVA values were significant to 0.005 or better. *P* values greater than 0.05 were considered not statistically significant.

ACKNOWLEDGMENTS

We thank M. Hermann for the preparation of cultures. The GFP-GluR1 carboxy tail construct was a gift from R. Malinow. This work was supported by the National Institute of Neurological Diseases and Stroke (36853), the Eye Institute (11116) and a Wellcome Trust Senior Fellowship to M.H.

COMPETING INTERESTS STATEMENT

The authors declare that they have no competing financial interests.

Received 16 December 2003; accepted 10 March 2004
Published online at http://www.nature.com/natureneuroscience/

1. Rivadulla, C., Sharma, J. & Sur, M. Specific roles of NMDA and AMPA receptors in direction-selective and spatial phase-selective responses in visual cortex. *J. Neurosci.* **21**, 1710–1719 (2001).
2. Daw, N.W., Stein, P.S. & Fox, K. The role of NMDA receptors in information processing. *Annu. Rev. Neurosci.* **16**, 207–222 (1993).
3. Myme, C.I., Sugino, K., Turrigiano, G.G. & Nelson, S.B. The NMDA-to-AMPA ratio at synapses onto layer 2/3 pyramidal neurons is conserved across prefrontal and visual cortices. *J. Neurophysiol.* **90**, 771–779 (2003).
4. Watt, A.J., van Rossum, M.C., MacLeod, K.M., Nelson, S.B. & Turrigiano, G.G. Activity coregulates quantal AMPA and NMDA currents at neocortical synapses. *Neuron* **26**, 659–670 (2000).
5. Umemiya, M., Senda, M. & Murphy, T.H. Behaviour of NMDA and AMPA receptor-mediated miniature EPSCs at rat cortical neuron synapses identified by calcium imaging. *J. Physiol.* **521**, 113–122 (1999).
6. McAllister, A.K. & Stevens, C.F. Nonsaturation of AMPA and NMDA receptors at hippocampal synapses. *Proc. Natl. Acad. Sci. USA* **97**, 6173–6178 (2000).
7. Groc, L., Gustafsson, B. & Hanse, E. Spontaneous unitary synaptic activity in CA1 pyramidal neurons during early postnatal development: constant contribution of AMPA and NMDA receptors. *J. Neurosci.* **22**, 5552–5562 (2002).
8. Muller, D., Joly, M. & Lynch, G. Contributions of quisqualate and NMDA receptors to the induction and expression of LTP. *Science* **242**, 1694–1697 (1988).
9. Kauer, J.A., Malenka, R.C. & Nicoll, R.A. A persistent postsynaptic modification mediates long-term potentiation in the hippocampus. *Neuron* **1**, 911–917 (1988).
10. Perkel, D.J. & Nicoll, R.A. Evidence for all-or-none regulation of neurotransmitter release: implications for long-term potentiation. *J. Physiol.* **471**, 481–500 (1993).

11. Liao, D., Hessler, N.A. & Malinow, R. Activation of postsynaptically silent synapses during pairing-induced LTP in CA1 region of hippocampal slice. *Nature* **375**, 400–404 (1995).
12. Heynen, A.J., Quinlan, E.M., Bae, D.C. & Bear, M.F. Bidirectional, activity-dependent regulation of glutamate receptors in the adult hippocampus *in vivo*. *Neuron* **28**, 527–536 (2000).
13. Lu, W. *et al.* Activation of synaptic NMDA receptors induces membrane insertion of new AMPA receptors and LTP in cultured hippocampal neurons. *Neuron* **29**, 243–254 (2001).
14. Clark, K.A. & Collingridge, G.L. Synaptic potentiation of dual-component excitatory postsynaptic currents in the rat hippocampus. *J. Physiol.* **482**, 39–52 (1995).
15. Bashir, Z.I., Alford, S., Davies, S.N., Randall, A.D. & Collingridge, G.L. Long-term potentiation of NMDA receptor-mediated synaptic transmission in the hippocampus. *Nature* **349**, 156–158 (1991).
16. Aniksztejn, L. & Ben-Ari, Y. Expression of LTP by AMPA and/or NMDA receptors is determined by the extent of NMDA receptors activation during the tetanus. *J. Neurophysiol.* **74**, 2349–2357 (1995).
17. Grosshans, D.R., Clayton, D.A., Coultrap, S.J. & Browning, M.D. LTP leads to rapid surface expression of NMDA but not AMPA receptors in adult rat CA1. *Nat. Neurosci.* **5**, 27–33 (2002).
18. Berretta, N. *et al.* Long-term potentiation of NMDA receptor–mediated EPSP in guinea-pig hippocampal slices. *Eur. J. Neurosci.* **3**, 850–854 (1991).
19. Xiao, M.Y., Karpefors, M., Niu, Y.P. & Wigstrom, H. The complementary nature of long-term depression and potentiation revealed by dual component excitatory postsynaptic potentials in hippocampal slices from young rats. *Neuroscience* **68**, 625–635 (1995).
20. Malinow, R., Mainen, Z.F. & Hayashi, Y. LTP mechanisms: from silence to four-lane traffic. *Curr. Opin. Neurobiol.* **10**, 352–357 (2000).
21. Turrigiano, G.G., Leslie, K.R., Desai, N.S., Rutherford, L.C. & Nelson, S.B. Activity-dependent scaling of quantal amplitude in neocortical neurons. *Nature* **391**, 892–896 (1998).
22. Pratt, K.G., Watt, A.J., Griffith, L.C., Nelson, S.B. & Turrigiano, G.G. Activity-dependent remodeling of presynaptic inputs by postsynaptic expression of activated CaMKII. *Neuron* **39**, 269–281 (2003).
23. Sjöström, P.J., Turrigiano, G.G. & Nelson, S.B. Rate, timing, and cooperativity jointly determine cortical synaptic plasticity. *Neuron* **32**, 1149–1164 (2001).
24. Liao, D., Scannevin, R.H. & Huganir, R. Activation of silent synapses by rapid activity-dependent synaptic recruitment of AMPA receptors. *J. Neurosci.* **21**, 6008–6017 (2001).
25. Oliet, S.H., Malenka, R.C. & Nicoll, R.A. Bidirectional control of quantal size by synaptic activity in the hippocampus. *Science* **271**, 1294–1297 (1996).
26. Bekkers, J.M. & Stevens, C.F. Presynaptic mechanism for long-term potentiation in the hippocampus. *Nature* **346**, 724–729 (1990).
27. Fitzjohn, S.M. *et al.* An electrophysiological characterisation of long-term potentiation in cultured dissociated hippocampal neurones. *Neuropharmacology* **41**, 693–699 (2001).
28. Banke, T.G. *et al.* Control of GluR1 AMPA receptor function by cAMP-dependent protein kinase. *J. Neurosci.* **20**, 89–102 (2000).
29. Lambolez, B., Ropert, N., Perrais, D., Rossier, J. & Hestrin, S. Correlation between kinetics and RNA splicing of alpha-amino-3-hydroxy-5-methylisoxazole-4-propionic acid receptors in neocortical neurons. *Proc. Natl. Acad. Sci. USA* **93**, 1797–1802 (1996).
30. Choi, S., Klingauf, J. & Tsien, R.W. Postfusional regulation of cleft glutamate concentration during LTP at 'silent synapses'. *Nat. Neurosci.* **3**, 330–336 (2000).
31. Renger, J.J., Egles, C. & Liu, G. A developmental switch in neurotransmitter flux enhances synaptic efficacy by affecting AMPA receptor activation. *Neuron* **29**, 469–484 (2001).
32. Alagarsamy, S., Sorensen, S.D. & Conn, P.J. Coordinate regulation of metabotropic glutamate receptors. *Curr. Opin. Neurobiol.* **11**, 357–362 (2001).
33. Hayashi, Y. *et al.* Driving AMPA receptors into synapses by LTP and CaMKII: requirement for GluR1 and PDZ domain interaction. *Science* **287**, 2262–2267 (2000).
34. Rao, A. & Craig, A.M. Activity regulates the synaptic localization of the NMDA receptor in hippocampal neurons. *Neuron* **19**, 801–812 (1997).
35. Barria, A. & Malinow, R. Subunit-specific NMDA receptor trafficking to synapses. *Neuron* **35**, 345–353 (2002).
36. Shi, S.H. *et al.* Rapid spine delivery and redistribution of AMPA receptors after synaptic NMDA receptor activation. *Science* **284**, 1811–1816 (1999).
37. O'Brien, R.J. *et al.* Activity-dependent modulation of synaptic AMPA receptor accumulation. *Neuron* **21**, 1067–1078 (1998).
38. Lissin, D.V. *et al.* Activity differentially regulates the surface expression of synaptic AMPA and NMDA glutamate receptors. *Proc. Natl. Acad. Sci. USA* **95**, 7097–7102 (1998).
39. Liu, S.Q. & Cull-Candy, S.G. Synaptic activity at calcium-permeable AMPA receptors induces a switch in receptor subtype. *Nature* **405**, 454–458 (2000).
40. Ehlers, M.D. Reinsertion or degradation of AMPA receptors determined by activity-dependent endocytic sorting. *Neuron* **28**, 511–525 (2000).
41. Selig, D.K., Hjelmstad, G.O., Herron, C., Nicoll, R.A. & Malenka, R.C. Independent mechanisms for long-term depression of AMPA and NMDA responses. *Neuron* **15**, 417–426 (1995).
42. Shi, S., Hayashi, Y., Esteban, J.A. & Malinow, R. Subunit-specific rules governing AMPA receptor trafficking to synapses in hippocampal pyramidal neurons. *Cell* **105**, 331–343 (2001).
43. Mu, Y., Ostuka, T., Horton, A.C., Scott, D.B. & Ehlers, M.D. Activity-dependent mRNA splicing controls ER export and synaptic delivery of NMDA receptors. *Neuron* **40**, 581–594 (2003).
44. Passafaro, M., Piech, V. & Sheng, M. Subunit-specific temporal and spatial patterns of AMPA receptor exocytosis in hippocampal neurons. *Nat. Neurosci.* **4**, 917–926 (2001).
45. Song, I. & Huganir, R.L. Regulation of AMPA receptors during synaptic plasticity. *Trends Neurosci.* **25**, 578–588 (2002).
46. Scannevin, R.H. & Huganir, R.L. Postsynaptic organization and regulation of excitatory synapses. *Nat. Rev. Neurosci.* **1**, 133–141 (2000).
47. Turrigiano, G.G. Homeostatic plasticity in neuronal networks: the more things change, the more they stay the same. *Trends Neurosci.* **22**, 221–227 (1999).
48. Bienenstock, E.L., Cooper, L.N. & Munro, P.W. Theory for the development of neuron selectivity: orientation specificity and binocular interaction in visual cortex. *J. Neurosci.* **2**, 32–48 (1982).
49. Kilman, V., van Rossum, M.C. & Turrigiano, G.G. Activity deprivation reduces miniature IPSC amplitude by decreasing the number of postsynaptic $GABA_A$ receptors clustered at neocortical synapses. *J. Neurosci.* **22**, 1328–1337 (2002).
50. Sjöström, P.J., Turrigiano, G.G. & Nelson, S.B. Neocortical LTD via coincident activation of presynaptic NMDA and cannabinoid receptors. *Neuron* **39**, 641–654 (2003).